Annealing-induced morphological changes in segmented elastomers

J. W. C. Van Bogart*, D. A. Bluemke and S. L. Cooper
Department of Chemical Engineering, University of Wisconsin, Madison, Wisconsin 53706, *USA*
(*Received* 29 *December* 1980)

Thermal analysis has been used to study annealing-induced ordering in segmented elastomers. Twelve segmented elastomers were studied each having approximately 50% by wt hard segment content. Seven general classes of materials were examined including polyether and polyester polyurethanes, polyether polyurethane–urea, and polyether–polyester. Materials were slow cooled (-10°C min^{-1}) from the melt to an annealing temperature (-10°, 20°, 60°, 90° or 120°C) where they were annealed (16, 12, 8, 6 or 4 days, respectively). Annealing was followed by slow cooling (-10°C min^{-1}) to -120°C after which a d.s.c. experiment was run. In general, annealing resulted in an endothermic peak at a temperature 20°–50°C above that of the temperature of annealing. This phenomenon was observed in both semicrystalline and amorphous materials. The closer the annealing endotherm was to a crystalline endotherm without exceeding it in temperature, the larger its size. Annealing endotherms resulted from hard or soft segment ordering. Only one annealing endotherm was observed for a given annealing history, even though in some materials hard and soft segments could exhibit annealing-induced morphological changes. Hard segment homopolymers were studied yielding results similar to the block polymers containing shorter sequences of the same material. This suggests that annealing-induced ordering is an intradomain phenomenon not associated with the interphase between domains, or necessarily dependent on the chain architecture of segmented elastomers.

INTRODUCTION

The molecular architecture of segmented elastomers results in microphase separation of the component segments in the solid state. Domains formed from glassy, or semicrystalline segments (hard segments) act as physical crosslinks and/or filler particles for viscous, or rubbery segments (soft segments). Such a morphology results in materials exhibiting a broad rubbery plateau at temperatures between the glass transition temperature (T_g) of the soft segment and the temperature of hard segment softening. This dissociation temperature of the hard segments may involve passing through the hard segment T_g or melting point, depending on whether the hard segment domain is amorphous or semicrystalline[1].

Earlier research on the subject of annealing segmented copolymers has been carried out by Cooper *et al.*[2–5], Jacques[6] and Wilkes *et al.*[7–11]. Hesketh *et al.*[5] studied morphological changes in segmented elastomers induced by annealing and quenching using differential scanning calorimetry (d.s.c.). Measurements taken immediately after quenching from the annealing temperature showed that the soft segment T_g was higher than that of the control (unannealed) material. Thus it was suggested that the applied thermal history promoted increased mixing of hard and soft segments. It was further noted[5] that the shift in T_g was smaller for those materials having crystalline hard segments. With increasing time after quenching, the soft segment T_g values decreased and approached an 'equilibrium' value. As a result of annealing, endotherms attributed to the disruption of long range ordering in the hard segment domains were observed at a temperature slightly above (10°–20°C) that of the annealing temperature. Furthermore, these endotherms could be shifted to higher temperatures and their peak height increased by use of higher annealing temperatures. However, the temperatures corresponding to positions of crystalline melting endotherms were independent of the annealing/quenching conditions investigated.

During storage at room temperature, following sample quenching, an endotherm, in the range 50°–80°C, appeared and was seen to shift to higher temperatures and grow in size with longer ageing times. This endotherm was attributed to structure developed in the material due to room temperature annealing.

The previous study of Hesketh *et al.*[5] primarily investigated the kinetics of annealing-induced ordering at high temperatures (120°–190°C). This contribution focusses attention on morphological changes produced by annealing at moderate temperatures (-10° to 120°C). The material variables considered in this study included variations in both hard and soft segment type, the study of systems containing semicrystalline and amorphous hard segments, and investigation of pure hard segment homopolymers.

EXPERIMENTAL

Polyether and polyester polyurethane, polyether polyurethane–urea, and polyether polyester materials constituted the materials investigated. Polyurethane hard segments were based on 4,4′-diphenyl methane diisocyanate (MDI) chain-extended with 1,4-butanediol (BD), 4,4′-dicyclohexyl methane diisocyanate (H_{12}MDI) chain-extended with 1,4-butanediol (BD), or piperazine (PZ) chain extended with 1,4-butanediol bischloroformate (BDBC). Longer sequences of MDI/BD hard seg-

* Present address: 3M, 3M Center, St. Paul, Minnesota 55144, USA

0032-3861/81/101428-11$02.00

ments are crystallizable. H_{12}MDI/BD hard segments tend to be amorphous as a fresult of the *cis–trans*, *cis–cis*, and *trans–trans* isomers which tend to be present in the synthesis of these cycloaliphatic polyurethanes. However, with attention to purification, the *trans–trans* isomer of H_{12}MDI can be isolated and used to make model semicrystalline polyurethanes. PZ/BDBC hard segments are highly crystalline, but are incapable of forming hydrogen bonds as the nitrogen of the urethane group is incorporated in the piperazine ring. The polyurethane–urea hard segment was based on 4,4′-diphenyl methane diisocyanate (MDI) chain extended with ethylene diamine (ED). Hard segments in the polyether polyester material were poly(tetramethylene terephthalate) (PTMT) oligomers. The schematic structures of the hard segment materials used in this study are shown in *Figure 1*.

Three types of soft segment materials were studied including two polyesters, poly(tetramethylene adipate) (PTMA) and polycaprolactone (PCL), and one polyether, poly(tetramethylene oxide) (PTMO). The schematic structures of the soft segment materials used in this study are shown in *Figure 2*.

In total, seven segmented polyurethanes were studied. Designation codes for each material were: ET for MDI/BD/PTMO, ES for MDI/BD/PTMA, UPCL for MDI/BD/PCL, HPCL for H_{12}MDI/BD/PCL, ETUU for MDI/ED/PTMO, BB for PZ/BDBC/PTMO, and H for PTMT/PTMO. Although all materials are characterized with respect to system type, hard segment content, average hard segment length, and soft segment molecular weight in *Table 1*, it is helpful to explain further the codes used in the designation of the materials. For ET (poly*ET*her) and ES (poly*ES*ther) materials, the first number following the system name refers to the wt % MDI, while the second number refers to the approximate soft segment molecular weight in thousands. For the UPCL (*U*nhydrogenated polyurethane, *P*oly-*C*apro*L*actone based), HPCL (*H*ydrogenated polyurethane, *P*oly*C*apro*L*actone based), and ETUU (poly*ET*her poly*U*rethane–*U*rea) designated materials, the number immediately following the system name refers to the soft segment molecular weight, while the series of three numbers following the dash refers to the molar ratios of soft segment polyol, the hard segment chain extender and hard segment unit used in preparing the materials. The two numbers following the BB (*B*road soft segment molecular weight distribution, *B*road hard segment molecular weight distribution) designation for the piperazine-based materials refer to the soft segment molecular weight in thousands and the average number of piperazine units per hard segment less one unit, respectively. Finally, the number following the H in the polyether polyester materials refers to the wt % hard segment.

All materials in this thermal analysis study had approximate hard segment contents of 50 wt% with the exception of the polyurethane–urea (ETUU) which had a hard segment content of 36%. Samples were prepared for study by compression moulding discs 31.8 mm in diameter and 1.3 mm thick. Moulding was carried out at a temperature 15°C higher than the highest d.s.c. endotherm of the bulk material for semicrystalline systems.

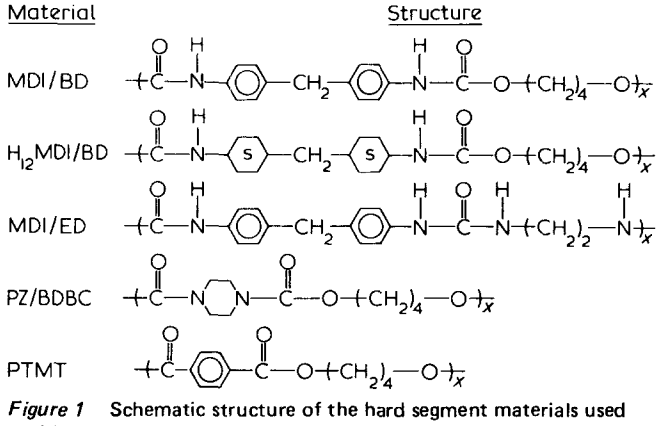

Figure 1 Schematic structure of the hard segment materials used in this study

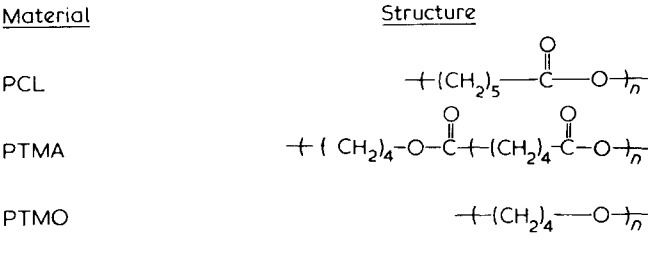

Figure 2 Schematic structure of the soft segment materials used in this study

Table 1 Sample characterization

Sample	System type	Wt % hard segment content	Average number of hard segment units per hard segment	Soft segment molecular weight
ET-38-1	MDI/BD/PTMO	46	2.86	980
ET-38-2	MDI/BD/PTMO	50	6	2000
ES-38-1	MDI/BD/PTMA	48	3.11	901
ES-38-2	MDI/BD/PTMA	54	7	1962
ES-38-5	MDI/BD/PTMA	54	15	4545
UPCL 830-123	MDI/BD/PCL	53	3	830
UPCL 2000-145	MDI/BD/PCL	45	5	2000
HPCL 830-123	H_{12}MDI/BD/PCL	54	3	830
HPCL 2000-145	H_{12}MDI/BD/PCL	46	5	2000
ETUU 1000-112	MDI/ED/PTMO	36	2	1022
BB-1,4	PZ/BDBC/PTMO	51	5	1003
H-49	PTMT/PTMO	49	4.8	1000

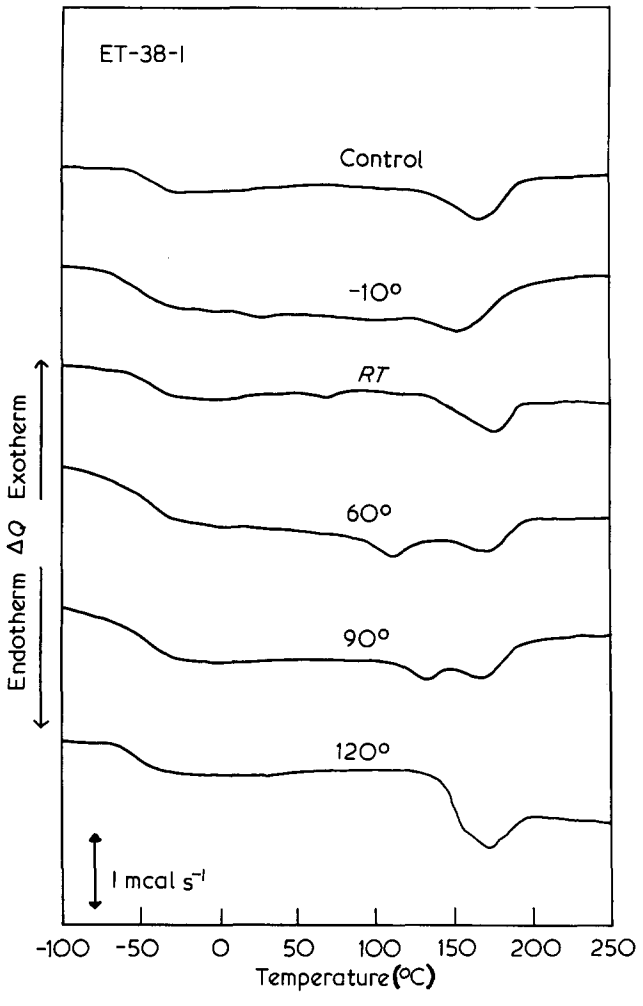

Figure 3 D.s.c. curves for ET-38-1. Temperatures of annealing are indicated. (*RT* = room temperature, 20°C)

Amorphous materials were moulded at a temperature 30°C higher than the glass transition temperature, T_g, of the hard segment of the bulk material.

Sample annealing was accomplished as follows. A 15.0 ±0.1 mg sample of each material was placed in a sealed d.s.c. pan. Samples of all 12 materials were then placed in a metal can flushed with nitrogen. The can containing the samples was placed in a rate-programmable oven set at 250°C. Samples were held at 250°C for 5 min and then cooled at a rate of 10°C min^{-1} to the annealing temperature desired at which time they were removed and placed in a holding oven set at the annealing temperature. Samples were annealed at −10°, 20° (room temperature, *RT*), 60°, 90° or 120°C for 16, 12, 8, 6 or 4 days, respectively. After annealing, each sample was transferred to the d.s.c. at the annealing temperature. Samples were then slow-cooled from the annealing temperature to −120°C at 10°C min^{-1}. A control of each material was prepared by heating the sample to 250°C in the d.s.c., holding for 5 min at that temperature (to erase thermal history) and then slow cooling at 10°C min^{-1} to −120°C. A thermogram of each sample was obtained using a Perkin–Elmer Model DSC-2 equipped with a scanning auto-zero accessory at a 20°C min^{-1} heating rate and a sensitivity of 5 mcal s^{-1} under a helium purge.

Samples of pure MDI/BD and H_{12}MDI/BD homopolymer were also prepared by compression moulding via the procedure outlined above. Half discs were then cut and annealed at 20°C (room temperature, *RT*), 60°, 90° and 120°C for H_{12}MDI/BD for 7, 3, 3 and 1 days, respectively, and at 20°, 60°, 90°, 120° and 150°C for 7, 3, 3, 1 and 1 days, respectively, for MDI/BD. Following annealing, samples were slow-cooled to room temperature where they were stored in a desiccator for at least 1 week. Control materials consisted of material slow cooled (−10°C min^{-1}) from the melt to −120°C and rerun in the d.s.c.

RESULTS AND DISCUSSION

Differential scanning calorimetry (d.s.c.) thermograms for the 12 materials studied are shown in *Figures 3–14* which correspond to the order of materials listed in *Table 1*. The materials studied can be categorized according to their domain microstructures. Thus representative samples can be found with semicrystalline hard and soft segment domains, only semicrystalline hard segment domains, only semicrystalline soft segment domains, or amorphous hard and soft segment domains. Materials showing crystallinity in both domains were ET-38-2, ES-38-5, and UPCL 2000-145. D.s.c. thermograms for these materials are shown in *Figures 4*, *7* and *9*, respectively. Quite a number of materials showed hard segment crystallinity only, including ET-38-1, ES-38-1, ES-38-2, UPCL 830-123, HPCL 2000-145, BB-1,4 and H-49 for which d.s.c.

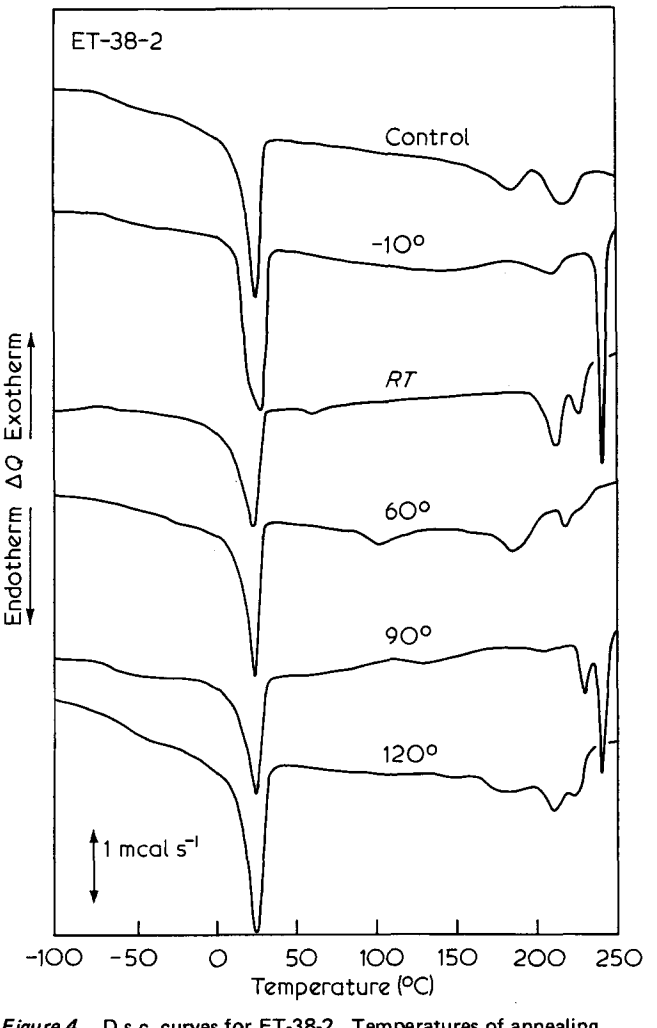

Figure 4 D.s.c. curves for ET-38-2. Temperatures of annealing are indicated. (*RT* = room temperature, 20°C)

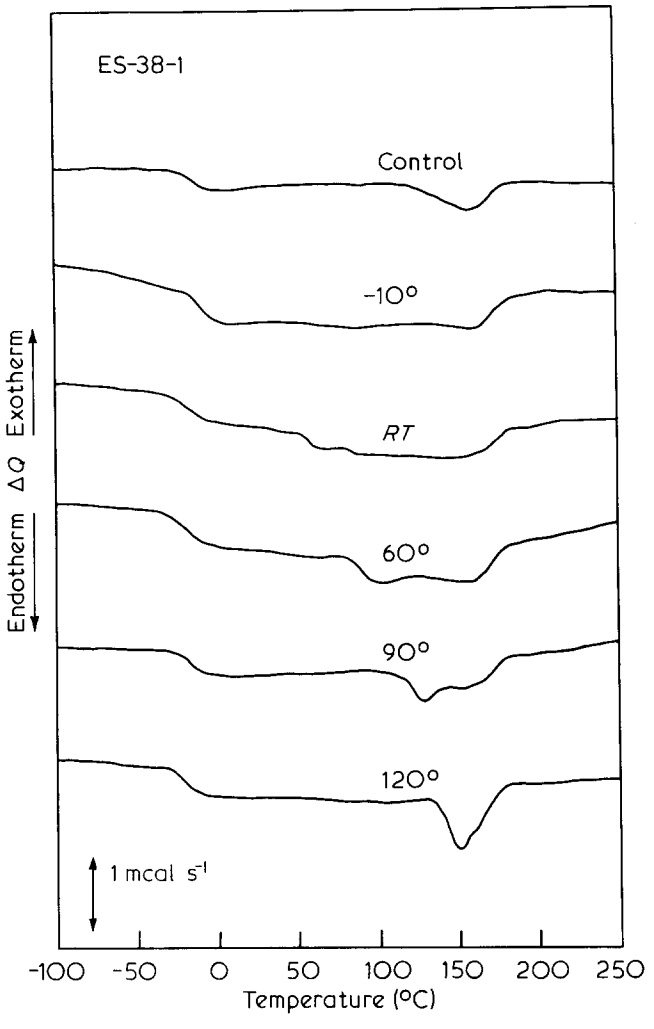

Figure 5 D.s.c. curves for ES-38-1. Temperatures of annealing are indicated. (*RT* = room temperature, 20°C)

traces are shown in *Figures 3, 5, 6, 8, 11, 13* and *14*, respectively. D.s.c. results for ETUU 1000-112, exhibiting only soft segment crystallinity, are shown in *Figure 12*. Finally, d.s.c. traces for HPCL 830-123, which is completely amorphous, are shown in *Figure 10*.

D.s.c. traces taken of the hard segment homopolymers, MDI/BD and H_{12}MDI/BD, are shown in *Figures 15* and *16*, respectively.

Before proceeding with a discussion of the annealed materials, some comment on the difference in the crystallizability of materials is of interest. If sufficiently long, crystallinity could be observed in all three families of soft segment materials studied. In general, soft segment crystallinity was not observed if the material had a soft segment molecular weight less than 1000. This observation holds for segmented polymers of about 50% hard segment. At lower hard segment content, the hard segment domains exert less of a filler effect and allow crystallization to occur at lower soft segment molecular weights if the soft segment is crystallizable.

Comparing UPCL 2000-145 with HPCL 2000-145, the former has a semicrystalline soft segment whereas the latter shows no evidence of soft segment crystallinity. The lack of soft segment crystallinity in HPCL 2000-145 could result from a greater hard segment/soft segment affinity due to the lower polarity of the hydrogenated hard segment which suppresses soft segment crystallinity through greater hard segment/soft segment mixing.

Table 2 lists soft segment glass transitions (T_g) for the materials studied. In cases where more than one soft segment molecular weight was studied for a given system, the soft segment T_g for the control materials can be seen to decrease with increasing molecular weight. A greater degree of phase separation allowed by the longer segment lengths results in greater phase purity and the lower T_gs observed[12].

The difficult crystallizability of the HPCL family hard segment has already been mentioned. As seen in *Figure 17*, the 4,4'-dicyclohexyl methane diisocyanate (H_{12}MDI) hard segment unit exists in three configurational isomeric forms. In preparation of a hard segment from this mixture of isomers, a random hard segment structure results which inhibits, but does not necessarily eliminate, crystallinity. Hard segments composed of the *trans–trans* isomer of H_{12}MDI exclusively, are crystalline so that if 2 or 3 adjacent *trans–trans* isomers are found along a hard segment chain backbone, some crystallinity can be realized. The MDI/BD hard segment has a regular repeat structure capable of a high degree of crystallinity.

Table 3 summarizes annealing endotherm peak positions as a function of annealing temperature for all the materials investigated. On the whole, an annealing endotherm can be observed at a temperature 20°–50°C higher than the temperature of annealing. Depending on the temperature of annealing, and whether or not the hard

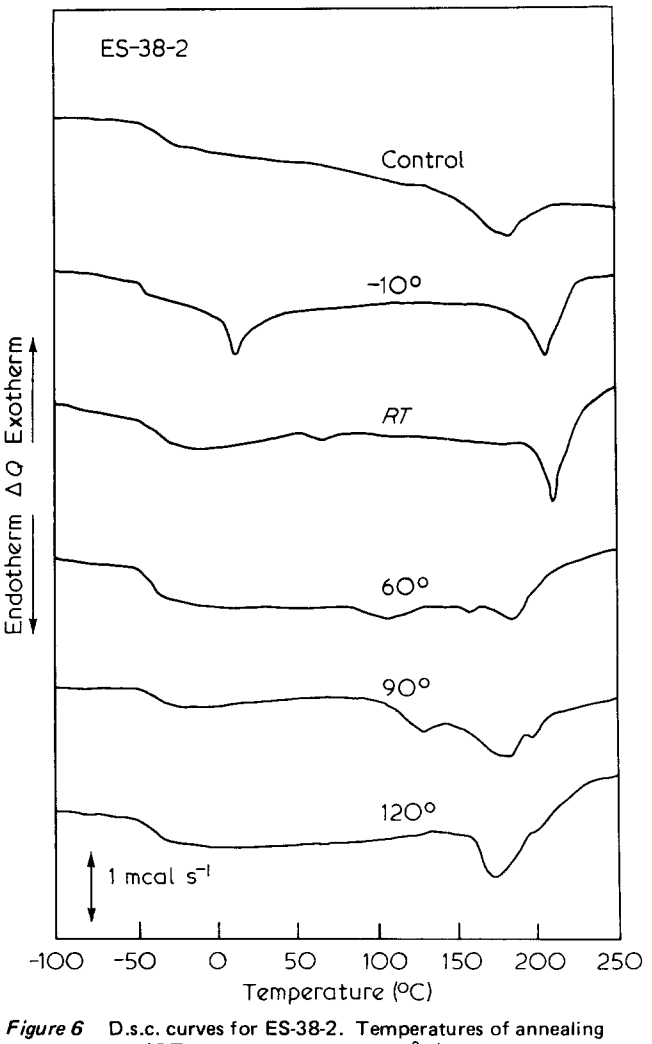

Figure 6 D.s.c. curves for ES-38-2. Temperatures of annealing are indicated. (*RT* = room temperature, 20°C)

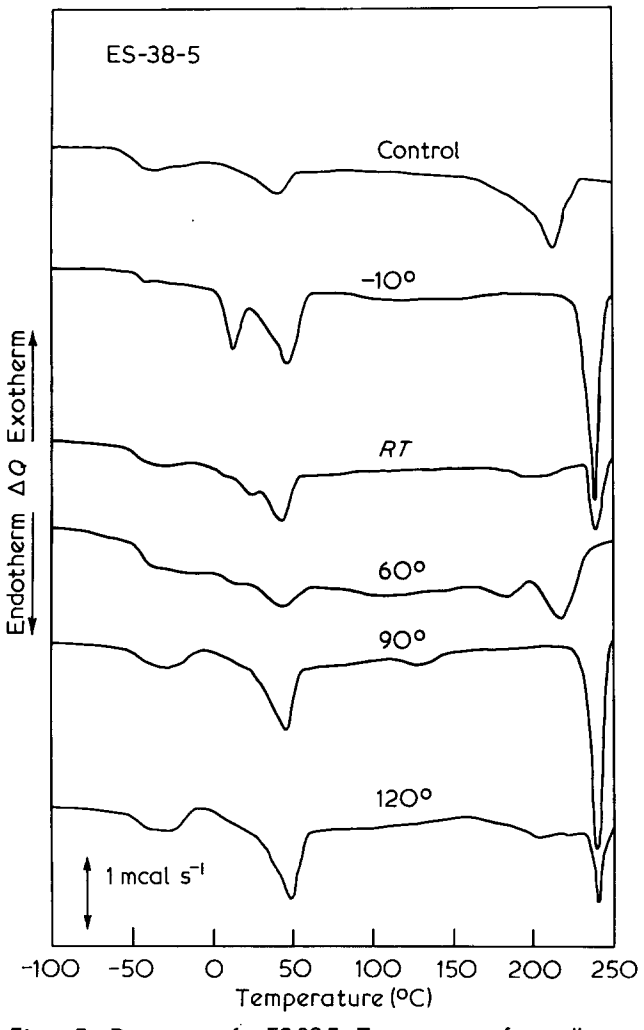

Figure 7 D.s.c. curves for ES-38-5. Temperatures of annealing are indicated. (*RT* = room temperature, 20°C)

segment and/or soft segment of the material was crystalline, the annealing endotherm varied in size and could be attributed to either (or both) hard or soft segment ordering.

A model to explain the annealing produced endotherms has been presented earlier by Cooper *et al.*[5]. Briefly, the annealing endotherms result from the disruption of ordered segments. Between the completely amorphous and perfectly crystalline states, there exists a continuum of ordered segment morphologies. Disruption of this ordering requires energy and thus an endotherm is observed. These endotherms occur at temperatures below the crystalline melting temperature, because the energies required for dissociation are lower, due to a lower degree of ordering than in crystalline systems.

When a sample is held at a given temperature, ordering which disrupts below the annealing temperature will be lost and those chain segments affected will exist in a fluid state. If at the annealing conditions the fluid segments are to frevert to a solid state structure, the segments must reorganize into an arrangement which will be stable at the annealing temperature. Thus, they may add to more stable, more ordered segments, functioning as nuclei in a process rather like recrystallization. It is also suggested that more stable orders may grow out of amorphous regions, thus increasing the number of ordered regions. The annealing endotherm, then, represents the dissolution of structure characteristic of the ordering produced by the annealing process. Higher annealing temperatures result in greater peak areas as more lower temperature structure is disrupted and reorganized with a higher degree of perfection.

The discussion of the experimental data begins with the simplest case—that of a completely amorphous material, HPCL 830-123. Annealing endotherms are observed in all cases up to 90°C. This demonstrates that hard or soft segment crystallinity is not a prerequisite for the observation of an annealing-induced ordering endotherm, or annealing peak. Annealing at 120°C, which is above the hard segment T_g of about 90°C, produces a thermogram similar to that of the control material. At this temperature, the high degree of molecular mobility allows no memory of thermal treatment to be retained.

Figure 12 shows the d.s.c. results for ETUU 1000-112 which has crystallinity in the soft segment. Annealing at −10°C did not result in an easily discernible annealing peak, but it did result in a sizeable increase in the degree of soft segment crystallinity. This is usually the case when annealing is done just below a melting point. In this case the annealing peak and the crystalline melting peak have merged. Annealing at room temperature resulted in a peak with a shoulder at 27°C. This resulted from soft segment crystallites which were large enough to be stable at the temperature of annealing. The portion of the peak occurring below 20°C, however, which constitutes most of

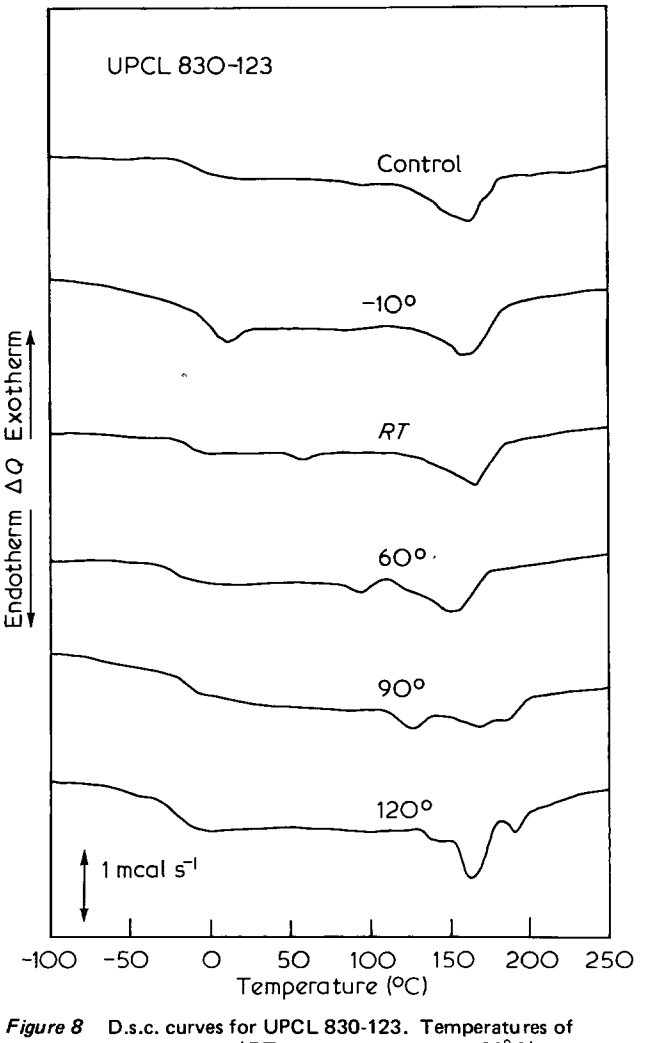

Figure 8 D.s.c. curves for UPCL 830-123. Temperatures of annealing are indicated. (*RT* = room temperature, 20°C)

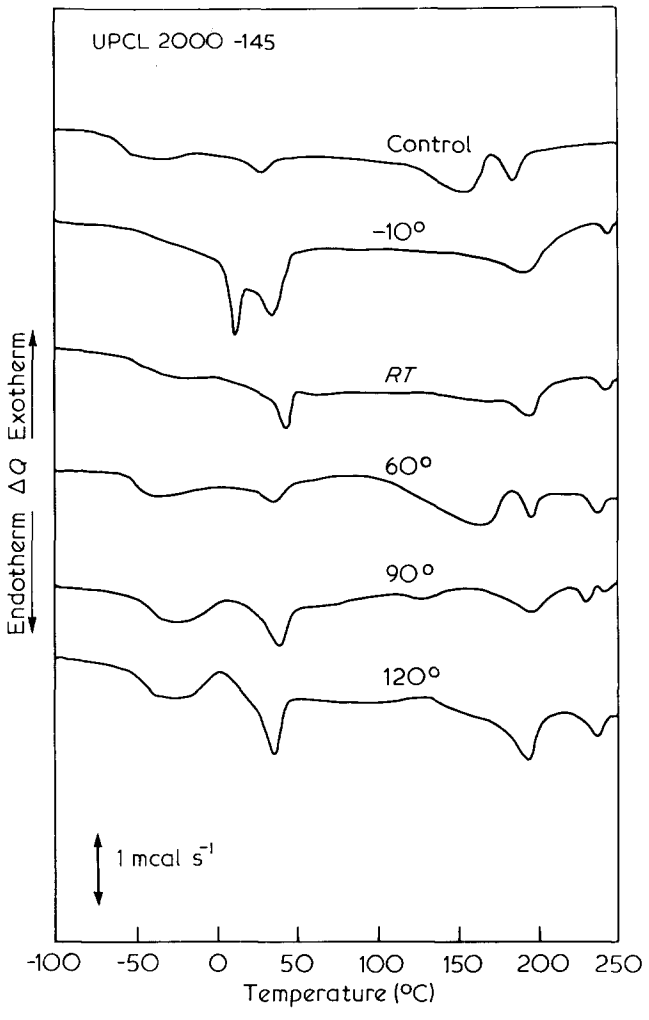

Figure 9 D.s.c. curves for UPCL 2000-145. Temperatures of annealing are indicated. (*RT* = room temperature, 20°C)

the peak, should have been disrupted at the annealing temperature. The exotherm corresponding to soft segment crystallization occurring at −7°C indicates that considerable crystallization of the soft segments occurred just before melting at 16°C. Thus the soft segments, with the exception of those constituting the peak shoulder at 27°C, were molten at the annealing temperature. It may be suggested that large soft segment crystallites existing at the annealing temperature acted as nuclei promoting crystallization both on cooling from 20°C and on subsequent reheating from the glassy state.

Another possiblity for the enhancement of peak size by room temperature annealing in ETUU 1000-112 could be the improvement in phase separation afforded by annealing. If this were the case, however, then similar results would be expected when annealing was performed at 60°C or above. This was not observed. This suggests that the glassy hard segment domains do not contribute to the retention of thermal history in the soft segment domains.

Proceeding to materials having semicrystalline hard segments only, the d.s.c. thermograms of ET-38-1, ES-38-1, ES-38-2, UPCL 830-123, HPCL 2000-145, BB-1,4, and H-49 shown in *Figures 3, 5, 6, 8, 11, 13*, and *14*, respectively should be considered. In general, an endothermic peak, ascribed to the disruption of ordered, but non-crystalline, hard segments, can be observed at a position 20°–50°C higher than the annealing temperature. This peak shifts to higher temperatures and grows in size as the annealing temperature is increased. In cases where the melting temperature of the hard segments was low enough, the annealing endotherm merged with the crystalline endotherm at the highest annealing temperature. In general, the size, shape, and position of the crystalline endotherms were unaffected by the annealing conditions, except where the annealing endotherm and the crystalline endotherm merged. In a comparison of materials, the size of the annealing peak varied inversely with the size of the crystalline endotherms. The fact that the BB-1,4 and H-49 materials exhibited behaviour analogous to the other materials in this group shows that the annealing-induced endotherms are not associated with hydrogen bonding[4] nor are they unique to the polyurethanes.

The size of the annealing endotherm is representative of the amount of material participating in the thermal event. In materials exhibiting high degrees of hard segment crystallinity, such as H-49, most hard segment material is incorporated in crystalline domains, so less is available for the ordered type of structure described earlier. In materials with low hard segment crystallinity, such as HPCL 2000-145, the opposite is true, and relatively large annealing endotherms are observed.

Within each material, the size of the annealing endotherm depends on its proximity to a crystalline endotherm. During annealing, hard segments coming from aggregations which are disrupted by the annealing con-

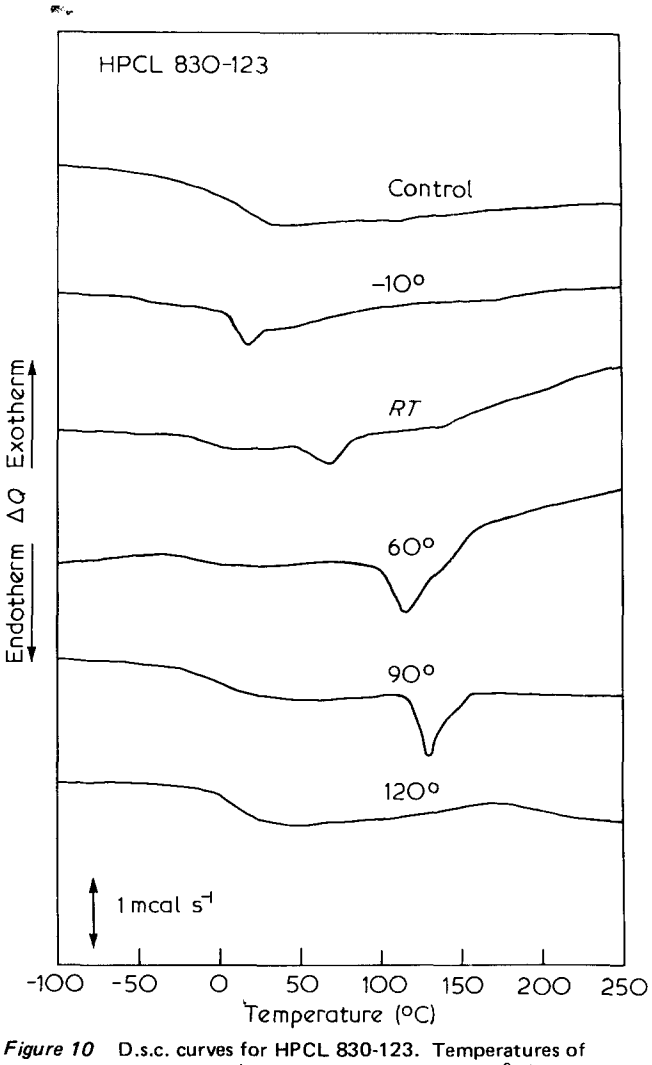

Figure 10 D.s.c. curves for HPCL 830-123. Temperatures of annealing are indicated. (*RT* = room temperature, 20°C)

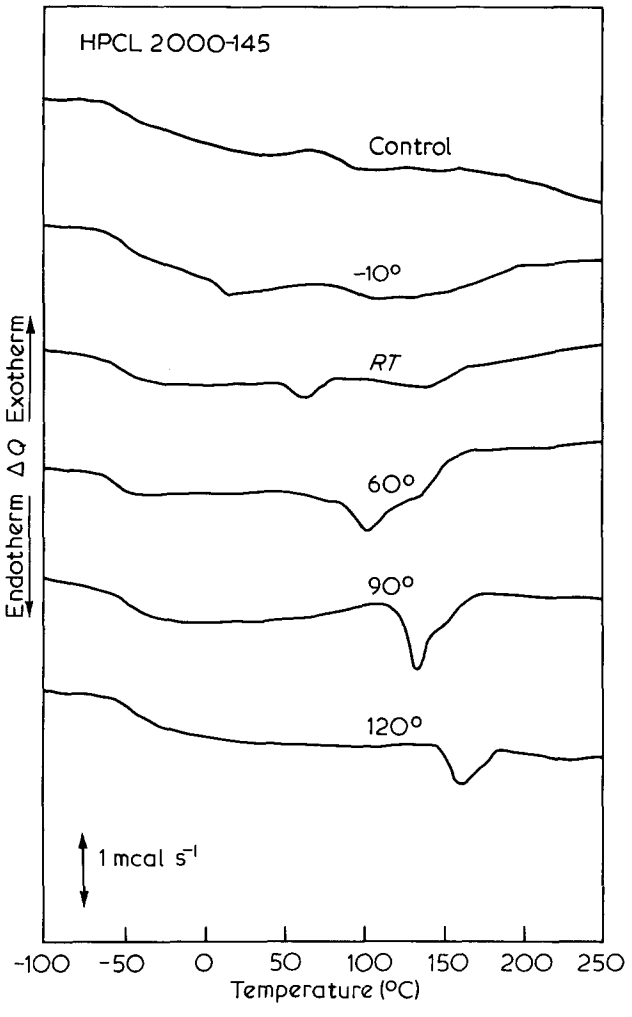

Figure 11 D.s.c. curves for HPCL 2000-145. Temperatures of annealing are indicated. (*RT* = room temperature, 20°C)

ditions reform into more closely packed, more highly ordered domains which dissociate at a temperature just above the annealing temperature. Thus the size of the annealing endotherm depends on the amount of material which dissociates at temperatures below the annealing temperature. A broad distribution of orders exists below the temperature of crystalline melting in the control materials. The range of ordering appears broad enough so that a specific peak need not be observed in the d.s.c. trace of the control[5]. Thus, the higher the annealing temperature, without exceeding the melting temperature, the greater the amount of material available for participation in an annealing-induced endotherm. This results in larger annealing peaks at higher annealing temperatures.

On the whole, the crystalline hard segment materials followed the aforementioned scenario although there were exceptions. In *Figure 6* which shows the d.s.c. results for ES-38-2, a substantially larger annealing endotherm is observed at 14°C following annealing at −10°C than that observed following annealing at room temperature. It is suggested that while in this case some hard segment material may participate in the formation of the annealing peak, annealing-induced soft segment aggregations predominate. It is of interest that in this case the annealing peak could reflect the disruption of two physically separate phenomenon—the dissociation of order in the hard segment phase and the soft segment order phase. The fact that the same temperature is observed for both phenomena may be fortuitous as it suggests that the position of the annealing-induced endotherm is a function only of annealing temperature and not of chemical structure.

Observing soft segment T_g data in *Table 2*, it is also clear that annealing ES-38-2 at −10°C (T_g = −45°C) results in a significant improvement in soft segment purity relative to the control (T_g = −36°C). Perhaps it is this improvement in phase purity which induces soft segment orders to form. Improvement in hard segment domain purity is also apparent as indicated by a shift of the hard segment crystalline endotherm to higher temperature.

Annealing ES-38-2 at 20°C results in an endotherm consistent with those observed at higher annealing temperatures, suggesting the absence of contributions from the soft segment domains. The absence of contributions from soft segment orderings in other materials of this class may have resulted from the lower soft segment molecular weights (approximately 1000) which may be too low to allow formation of polyester crystallites.

UPCL 830-123 (*Figure 8*) shows an enhanced annealing-induced endotherm after annealing at −10°C. In this case, because of the proximity of the soft segment T_g (approximately −15°C) to the annealing temperature, the observed phenomenon is enhanced to some degree by enthalpy relaxation in the soft segment. This was not observed in other polyurethanes because of their lower soft segment T_gs.

The annealing-induced endotherm of HPCL 2000-145

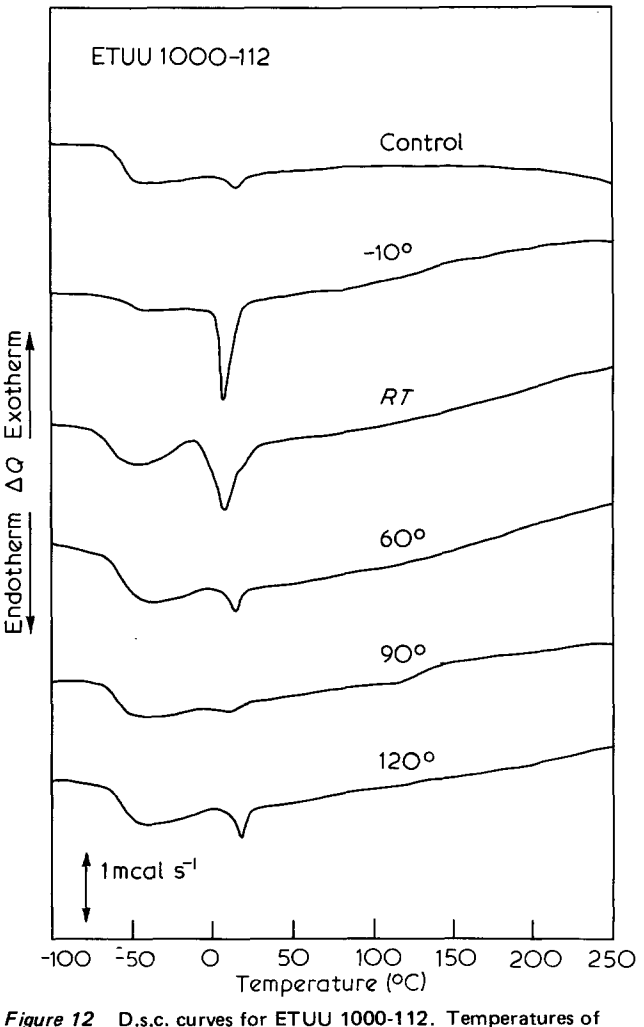

Figure 12 D.s.c. curves for ETUU 1000-112. Temperatures of annealing are indicated. (*RT* = room temperature, 20°C)

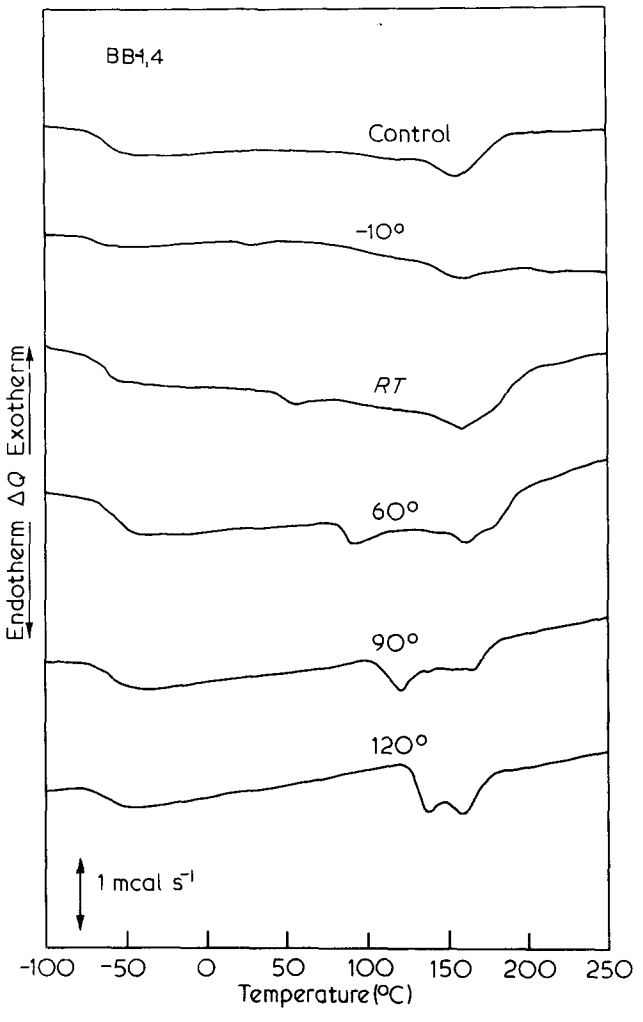

Figure 13 D.s.c. curves for BB-1,4. Temperatures of annealing are indicated. (*RT* = room temperature, 20°C)

(*Figure 11*) increases in size with annealing temperature up to 90°C and then decreases in size for annealing at 120°C. In this polymer, it is possible that sequences of *trans* H_{12}MDI/BD hard segments may be crystallizable. Although subsegments formed from the *cis–cis* and *cis–trans* isomers of H_{12}MDI are incapable of crystallizing, they may be allowed to participate in lesser ordered, non-crystalline aggregations for which a d.s.c. endotherm is observable. The former crystalline orders will persist up to the crystalline melting temperature, whereas the latter orders will dissociate at temperatures exceeding the T_g of the hard segment material. Such traits are unique to the H_{12}MDI/BD hard segment in this study as all other hard segments, if of sufficient length and given sufficient opportunity, will crystallize.

The three remaining materials studied, ET-38-2, ES-38-5, and UPCL 2000-145, all exhibited both semicrystalline hard and soft segment behaviour as seen in *Figures 4*, *7*, and *9*, respectively. In these materials, both hard and soft segment materials participate in forming the annealing-induced morphologies giving rise to the annealing endotherm. One feature of these data is that in highly crystalline samples the annealing endotherm size is significantly reduced and even unobservable in some cases. As most hard and soft segment material is incorporated in crystalline domains in these materials, less is available for the ordered type of structure as discussed earlier. It is also observed that the effect that the annealing process has on a sample depends on the annealing temperature's proximity to a crystalline melting temperature. Annealing sample ES-38-5 (*Figure 7*) at −10°C results in an annealing peak of significant size below the crystalline soft segment melting peak. Furthermore, the crystalline soft segment peak shows an increase in size as a result of annealing. An unexpected result was the increase in the size and temperature of the hard segment crystalline melting peak. Apparently, the improvement of soft segment structure brought about by annealing improves the degree of phase separation of the overall material, thus enhancing hard segment crystallinity. Such an effect was observed in the d.s.c. trace for ES-38-2 annealed at −10°C (*Figure 6*). Increasing the annealing temperature to 60°C, a temperature above the soft segment melting temperature and relatively far from the hard segment melting temperature, results in thermal characteristics quite similar to those of the control material. Further increasing the annealing temperature to 90°C results in improved hard segment crystallinity. Here, improvement in hard segment crystallinity increases the degree of phase separation and so enhances soft segment crystallinity as shown by the larger soft segment melting peak height. Analogous results are observed for ET-38-2 (*Figure 4*) and UPCL 2000-145 (*Figure 9*).

One would expect that the improvement in phase separation seen as a result of annealing at −10° and 90°C would be reflected by a decrease in the soft segment T_g. From the data for ET-38-2, ES-38-5, and UPCL 2000-145

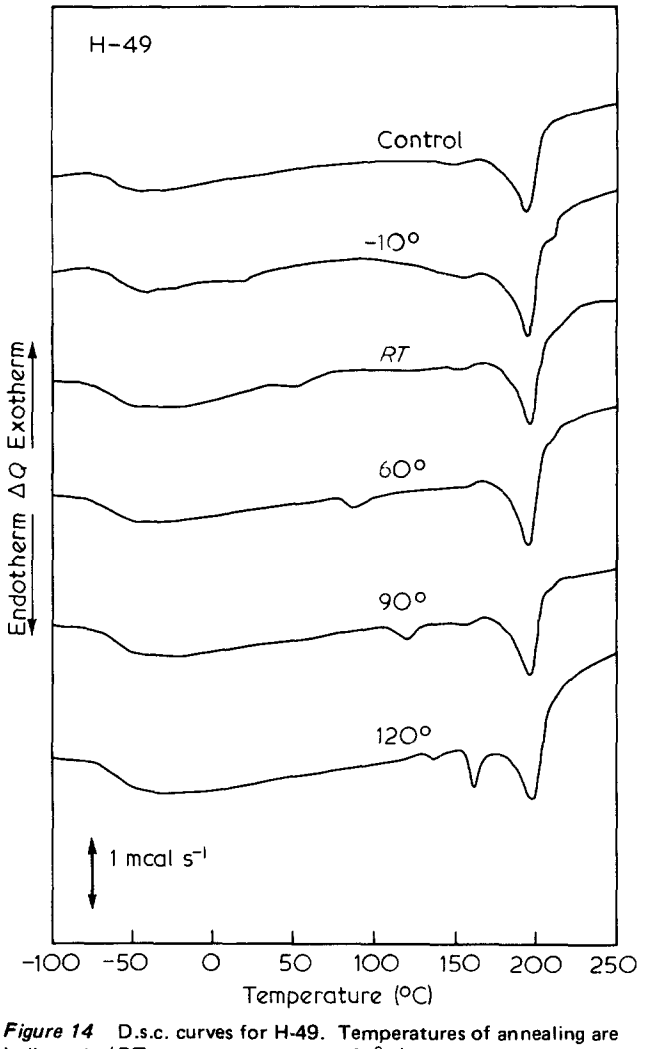

Figure 14 D.s.c. curves for H-49. Temperatures of annealing are indicated. (*RT* = room temperature, 20°C)

given in *Table 2*, however, this is not the case. Apparently, overall phase purity is improved upon annealing whereas the purity of specific amorphous regions within the soft segment domains remains about the same so that the soft segment T_g remains relatively constant.

ES-38-5 and ET-38-2 are unusual in that they show a higher degree of hard segment crystallinity after annealing at 90°C than after annealing at 120°C, even though the extent of soft segment crystallinity is improved by annealing at the higher temperature, perhaps prompted as a result of improved phase spearation. Possibly a slight thermal degradation of the hard segments at this temperature is the cause of the observed reduction in hard segment crystallinity. In contrast, UPCL 2000-145 shows an increase in hard and soft segment crystallinity in response to annealing at 120°C.

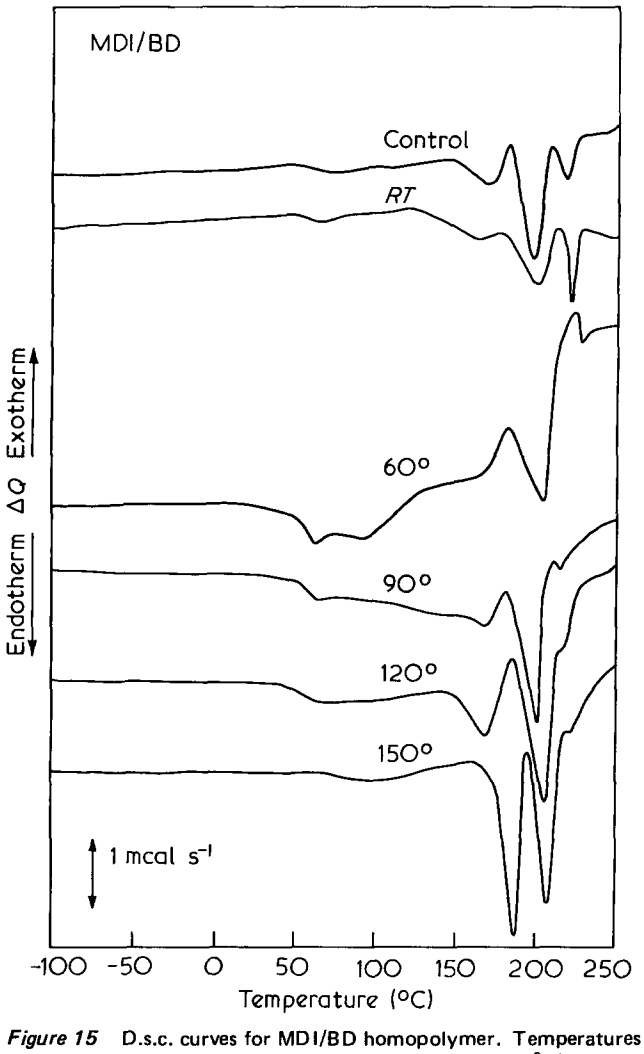

Figure 15 D.s.c. curves for MDI/BD homopolymer. Temperatures of annealing are indicated. (*RT* = room temperature, 20°C)

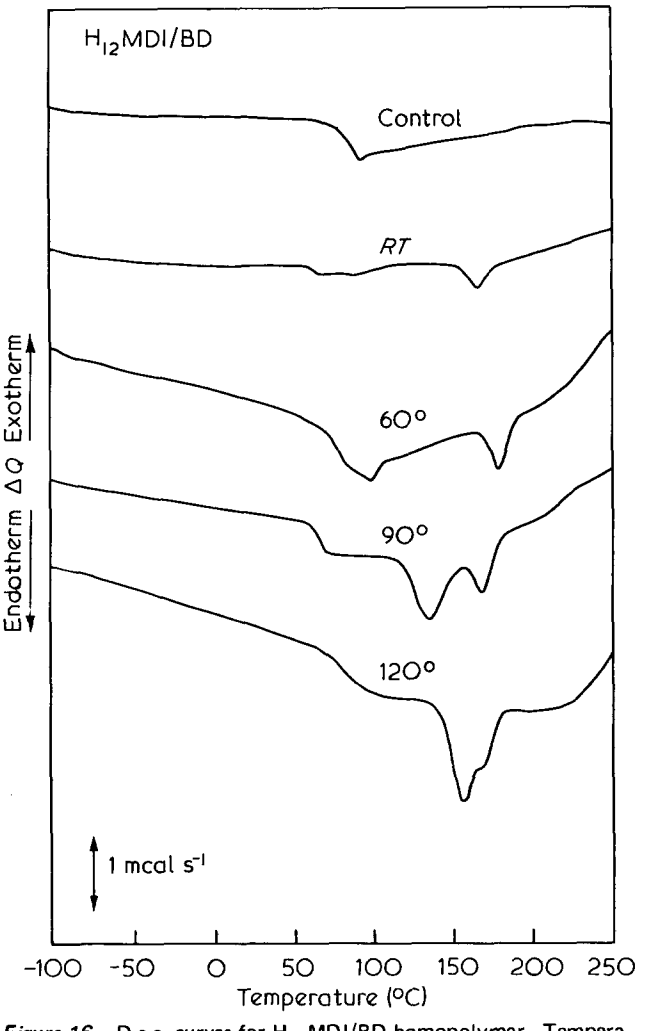

Figure 16 D.s.c. curves for H_{12}MDI/BD homopolymer. Temperatures of annealing are indicated. (*RT* = room temperature, 20°C)

Table 2 Soft segment glass transition temperature as a function of annealing temperature for segmented copolymer materials

Sample	Control (°C)	−10 (°C)	20 (°C)	60 (°C)	90 (°C)	120 (°C)
ET-38-1	−43*	−51	−45	−43	−40	−45
ET-38-2	−63	−63	–	–	−61	−53
ES-38-1	−12	−10	−14	−13	−14	−17
ES-38-2	−36	−45	−36	−40	−38	−36
ES-38-5	−46	−45	−43	−44	−45	−46
UPCL 830-123	−15	–	−13	−17	−12	−14
UPCL 2000-145	−40	–	−43	−42	−41	−43
HPCL 830-123	12	8	1	−15	10	12
HPCL 2000-145	−53	−52	−44	−53	−50	−52
ETUU 1000-112	−55	−53	−53	−52	−56	−57
BB-1,4	−60	−62	−61	−53	−57	−61
H-49	−57	−59	−59	−59	−57	−58

* Uncertainty for each temperature is ±2°C

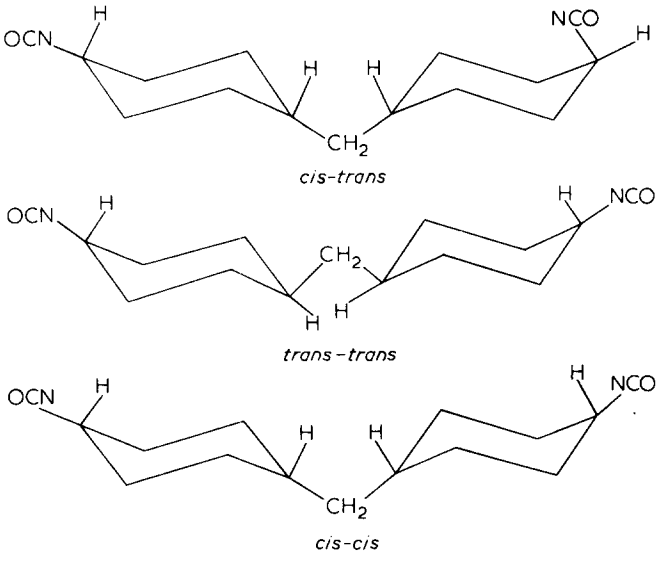

Figure 17 Configurational isomers of 4,4'-dicyclohexyl methane diisocyanate (H_{12}MDI)

Table 3 Annealing endotherm temperature as a function of annealing temperature for segmented copolymer materials

Sample	−10 (°C)	20 (°C)	60 (°C)	90 (°C)	120 (°C)
ET-38-1	30*	65	106	130	160
ET-38-2	26	58	101	130	150
ES-38-1	–	66	99	129	158
ES-38-2	14	64	108	128	145
ES-38-5	14	–	98	124	–
UPCL 830-123	14	61	96	126	140
UPCL 2000-145	13	63	82	135	143
HPCL 830-123	18	66	106	129	–
HPCL 2000-145	17	67	80	127	143
ETUU 1000-112	11	–	–	112(?)	–
BB-1,4	23	56	91	123	138
H-49	10	53	88	120	136

* Uncertainty for each temperature is ±2°C

Annealing ES-38-5 and ET-38-2 at 90° and 120°C results in soft segment recrystallization prior to soft segment melting. Normally this phenomenon is seen in only quenched materials. The improvement in phase separation brought about by annealing of these materials may reduce the concentration of nucleating agents in the soft segment so that upon slow cooling from the annealing temperature (-10°C min^{-1}) the soft segment is supercooled as a glass rather than forming a crystalline structure. It is not until reheating in the d.s.c. that nucleation and crystal growth occurs.

In a complementary study, pure hard segment homopolymer materials of MDI/BD (*Figure 15*) and H_{12}MDI/BD (*Figure 16*) were also annealed and examined by thermal analysis. Positions of the observed annealing peaks are listed in *Table 4*. Results are analogous to those observed for the materials exhibiting hard segment crystallinity only. However, because the homopolymers were stored at room temperature prior to analysis, a room temperature annealing endotherm can also be observed at approximately 65°C.

The similarity of hard segment ordering in both the segmented copolymer materials and the homopolymers indicates that the annealing-induced ordering is not dependent on the presence of a soft segment phase. For example, annealing MDI/BD at room temperature results in an annealing peak even though the material is below its T_g. Thus hard segment ordering is possible without the presence of a soft segment rubbery phase acting in such a way as to enhance mobility. The presence of annealing-induced ordering in hard segment homopolymer also indicates that the phenomenon need not be ascribed to the hard domain–soft domain interfacial region (approximately 5–10 Å thick[13,14]) present in the segmented copolymers.

For the H_{12}MDI/BD material (*Figure 16*), two peaks are found above the glass transition temperature. These peaks are probably the result of the break-up of *trans-trans* microcrystalline regions. The lower temperature peak results from the annealing conditions whereas the higher temperature peak results from the fact that this family of materials were all moulded at 150°C. For the MDI/BD materials (*Figure 15*), the high temperature endotherms also result from the melting of hard segment crystallites.

CONCLUSIONS

A systematic study of annealing-induced ordering in a variety of segmented polyurethanes has been accomplished using differential scanning calorimetry. In general, annealing resulted in an endothermic peak at a temperature 20°–50°C above that of the temperature of annealing. This annealing endotherm was ascribed to the disruption of ordered segments—structure resulting from the reorganization of lesser segment orders into more perfect arrangements upon annealing. Annealing endotherms were observed in both semicrystalline and amorphous materials and could originate from either hard or soft segment domain structure depending on the thermal history of the sample.

Only one annealing endotherm was observed in each material at each annealing temperature, even if both hard and soft segment orders were known to contribute to the observed phenomenon. In materials where both segment types were crystallizable, improvement in the degree of crystallinity of one phase as a result of annealing, resulted in enhanced crystallinity of the other phase. In general, annealing at higher temperatures resulted in larger annealing endotherms, unless the temperature of annealing exceeded that of crystalline segment melting.

Similar annealing effects were observed in pure hard segment materials indicating that they did not depend on a segmented-elastomer-type architecture for development. This suggests that the annealing-induced ordering originated within the domain microstructure rather than being related to morphological changes associated with the interphase between domains.

Table 4 Annealing endotherm temperature as a function of annealing temperature for hard segment homopolymer materials

Sample	20 (°C)	60 (°C)	90 (°C)	120 (°C)	150 (°C)
MDI/BD	57*	94	128	172	188
H_{12}MDI/BD	72	100	135	156	NA

* Uncertainty for each temperature is ±2°C
NA Not applicable

ACKNOWLEDGEMENTS

The authors wish to thank the following individuals for supplying the materials used in this study: Dr E. A. Collins of the Diamond Shamrock Company who supplied the ET and ES series material during his association with B. F. Goodrich; Dr James C. West of Allied Chemical Corporation who synthesized the UPCL series material while a postdoctoral fellow at the University of Wisconsin; Laura E. Lerner who synthesized the HPCL based polymers for her MSc Thesis at the University of Wisconsin; Dr Charles S. Schollenberger of the B.F. Goodrich Company who supplied the ETUU material; Dr Lamar L. Harrell Jr. of E. I. DuPont de Nemours and Company who sent us the piperazine material; and Dr Gerald M. Estes of the E. I. DuPont de Nemours and Company who gave us the segmented polyester material. The authors wish to acknowledge support of this work by the polymer programme of the National Science Foundation through Grant DMR 78-11662.

REFERENCES

1 Van Bogart, J. W. C., Lilaonitkul, A. and Cooper, S. L. *Adv. Chem. Ser.* 1979, **176**, 3
2 Seymour, R. W. and Cooper, S. L. *J. Polym. Sci. (Polym. Lett. Edn.)* 1971, **9**, 689
3 Seymour, R. W. and Cooper, S. L. *Macromolecules* 1973, **6**, 48
4 Ng, H. N., Allegrezza, A. E., Seymour, R. W. and Cooper, S. L. *Polymer* 1973, **14**, 255
5 Hesketh, T. R., Van Bogart, J. W. C. and Cooper, S. L. *Polym. Eng. Sci.* 1980, **20**, 190
6 Jacques, C. H. M. in 'Polymer Alloys: Blends, Blocks, Grafts, and Interpenetrating Networks', (Eds. Daniel Klempner and Kurt Frisch) Plenum Press, New York, NY 1977, Polymer Science and Technology, Vol 10, p 287
7 Samuels, S. L. and Wilkes, G. L. *J. Polym. Sci. (A-2)* 1973, **11**, 807
8 Wildnauer, R. and Wilkes, G. L. *Polym. Prepr.* 1975, **16**, 600
9 Wilkes, G. L., Bagrodia, S., Humphries, W. and Wildnauer, R. *J. Polym. Sci. (Polym. Lett. Edn.)* 1975, **13**, 321
10 Wilkes, G. L. and Wildnauer, R. *J. Appl. Phys.* 1975, **46**, 4148
11 Wilkes, G. L. and Emerson, J. A. *J. Appl. Phys.* 1976, **47**, 4261
12 Krause, S. in 'Block and Graft Copolymers', (Eds. John J. Burke and Volker Weiss), Syracuse University Press, Syracuse, New York, 1973, p 143
13 Van Bogart, J. W. C., Lerner, L. E., West, J. C. and Cooper, S. L. *ACS Org. Coatings and Plastics Chem. Prepr.* 1979, **40**, 647
14 Van Bogart, J. W. C., Lilaonitkul, A., Lerner, L. E. and Cooper, S. L. *J. Macromol. Sci. (B)* 1980, **17**, 267